Comparison of Detailed Land Cover Mapping Based on SNI Classification Scheme using Conventional and Machine Learning Multispectral Classification

Fahrezi, A.,[1*] Danoedoro, P.[2] and Kamal, M.[2]
[1]Remote Sensing Graduate Study Program, Universitas Gadjah Mada, Indonesia
E-mail: agilakbarfahrezi@mail.ugm.ac.id
[2]Geographic Information Science Department, Universitas Gadjah Mada, Indonesia
**Corresponding Author*

DOI: https://doi.org/10.52939/ijg.v21i2.3941

Abstract
Accurate and efficient land cover mapping remains a critical challenge in remote sensing, particularly when adhering to standardized classification schemes. In Indonesia, the Standar Nasional Indonesia (SNI) 7645-1:2014 classification scheme serves as the national standard for land cover mapping but is inherently complex, having been designed for visual interpretation, rather a digital classification approach. This study attempted to applied the SNI classification scheme for digital image classification by comparing the result of two commonly used algorithm in digital image classification, namely Maximum Likelihood (ML) and Random Decision Forest (RDF). Based on preliminary land cover map and fieldwork conducted, we successfully identified 18 land cover classes based on SNI classification scheme with the scale of 1:250.000. Because single date imagery and spectral information were only used, modification to the classification is conducted by grouping the classes into a new class based on its basis land cover type. Due to various spectral response of classes, the imagery is classified into 29 classes which later will be combine in the post processing process. Aside from the percent correct, the quantity disagreement and allocation disagreement were also used for assessing the result of both algorithms. Accuracy assessment of the land cover maps shows 81.17% overall accuracy for ML algorithm and 82.92% for the RDF algorithm. The ML algorithm shows higher allocation disagreement, compared to RDF algorithm, indicating higher miss-classification were detected in the ML algorithm. On the other hand, RDF algorithm shows higher quantity disagreement, indicating that this algorithm overestimated the land cover produced. This approach served as an alternative approach for mapping land cover using the SNI classification scheme, aside from the established approached.

Keywords: Accuracy, Land Cover, ML, RDF, SNI Classification Scheme

1. Introduction

Accurate land cover maps play an important role in various studies, such as environmental and natural resource management, regional development, climate studies, and food security [1]. Remote sensing has been utilized as main data source for most land cover mapping ever since the launch and operation of Earth Resource Technology Satellite (ERTS), also known as Landsat-1 [2]. Advances in remote sensing platforms, computer processing, and integration with other data sources have increased attention on land cover mapping [3]. A significant issue in contemporary studies of land cover mapping is the challenge of deriving accurate and detailed land cover maps [4].

Many factors influence the accuracy of land cover maps, one of which is the classification scheme used to create the map. Several studies show that aside from data processing and classification, the choice of classification scheme significantly influence the accuracy of land cover maps [5][6] and [7]. Classification schemes are usually created for specific purposes, therefore lead to mismatches between existing maps, even if they depict the same information. This issue is common in Indonesia, resulting in difficulties of producing detailed and versatile land cover map. Indonesia has a wet tropical climate with diverse landscape and complex land cover.

The diverse landscape supports many different natural ecosystems and supports various socio-economic activities [8].

Therefore, some notable classification schemes, such as USGS, are not always compatible to represent the complex phenomena [9]. The USGS classification system were resource oriented, therefore did not included various human activity related land cover [10]. As a developing nation, Indonesia's land cover is significantly shaped by human activities, particularly in agricultural and urban contexts. For example, rice field in Indonesia were often mixed with other crops or subjected to rotations with other crops. Therefore, several land cover and land use classification scheme were developed in Indonesia [4][11] and [12]. In addition, the Indonesia Geospatial Agency (*Badan Informasi Geospasial*/BIG) has standardized LULC through the SNI (*Standar Nasional Indonesia*) 7645-1:2014, aiming to incorporate multiple sectoral perspectives [13].

SNI is specifically designed for visual interpretation to effectively represent the complexity of land cover in Indonesia. SNI also mixed land cover and land use terminology, although the difference between the two are clearly stated. This classification scheme is divided into three scales, namely 1:1000000, 1:250000 and 1:50000 or 1:25000. The 1:50,000 or 1:25,000 scales include a total of 103 classes. The 1:1000000 scale includes 8 classes and the 1:250,000 scale includes 36 classes. The 1:50,000 or 1:25,000 scales were explicitly stated to be a mixed between land use and land cover, while the two other scales are predominantly land cover classes. SNI classification scheme is created by separating predominantly vegetated and non-vegetated land. Vegetated and non-vegetated land cover types are further differentiated based on the degree of human intervention. Human intervention resulted in utilized/unutilized non vegetated land, and cultivated/non-cultivated vegetated land. Human intervention results in the classification of non-vegetated land into utilized and unutilized categories, and vegetated land into cultivated and non-cultivated categories. These classifications are then subdivided into more detailed land cover types, reflecting natural, semi-natural, or anthropogenic characteristics [6] and [10].

Because of the detailed categorization, specific approach has been developed to effectively map land cover using this scheme. One of them is landscape ecology approach, developed by [6], which relied on ecological aspect of the landscape and its relation with land cover. This approach is conducted in a form of visual interpretation, although digital image processing is still required to derive the parameters to support landscape ecological analysis. This approach required comprehensive understanding of landscape ecology and its relation with land cover, in addition to land cover interpretation expertise. Since SNI classification was designed for visual interpretation, application of digital image classification for this classification scheme remained an intriguing subject.

In this study, two approaches in digital image classification, namely the parametric (also known as conventional approach) and nonparametric, will be evaluated for land detailed land cover mapping using Landsat 8 multispectral data. We used a 1:250000 scale level in SNI classification to derived the land cover map. Both the Maximum Likelihood (ML) and Random Decision Forest (RDF) classification algorithms, representing parametric and nonparametric approach respectively, will be applied. These algorithms are regarded as among the best algorithm in their respective approaches, although RDF's status remains the subject of debate. The ML algorithm are regarded to have a more acceptable statistical background, in respect to other parametric classification, resulting in better performance and higher accuracy [14] and [15]. In term of RDF algorithm, result may still vary, but some studies mentioned that RDF are more capable to handle more complex land cover and resulted in higher accuracy compared to other nonparametric approach [16][17] and [9]. Both approaches will be employed to provide a deeper understanding of the performance of digital image classification when applied using the SNI classification, which was designed for visual interpretation. Many studies have suggested that nonparametric approach yields higher accuracy compared to parametric approach.

However, on this study, we have chosen not to assume that the nonparametric approach will result in higher accuracy; therefore, both approaches will be evaluated objectively. Additionally, we will only use multispectral data, ensuring an equal dataset for both approaches. The resulting land cover map will be evaluated using the error matrix and compared visually.

2. Materials and Methods

2.1 Location and Workflow

This research is conducted in southern part of Garut Regency, West Java Province, Indonesia. This location features a highly complex landscape, characterized of volcanic, denudational, fluvial, structural, marine, and aeolian landforms.

The diverse landforms combined with various socio-economic activities, contributes to a complex land cover within a relatively small area, making it well-suited for land cover mapping using the SNI classification scheme. The location will be bordered by an imaginary bounding box shown by the red box in Figure 1. Workflow in this study in shown in Figure 2. The workflow consists of four main steps, which is imagery preparation (green box), land cover mapping preparation (yellow box), land cover mapping (blue box), and comparison analysis (orange box).

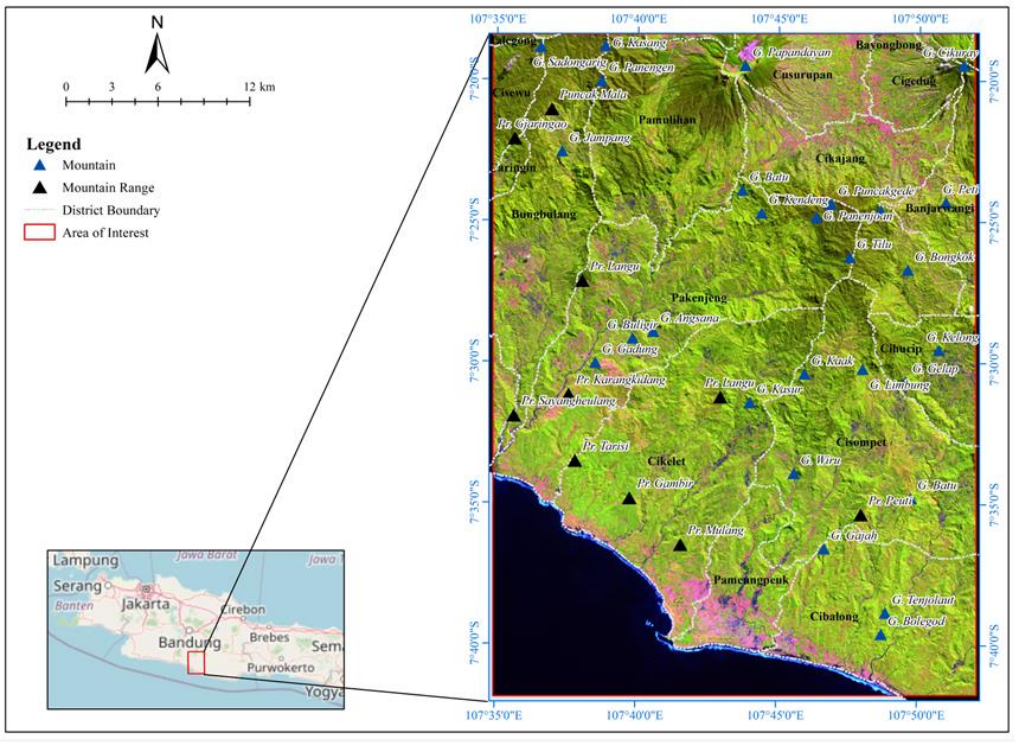

Figure 1: Southern Garut Regency, West Java Province, Indonesia

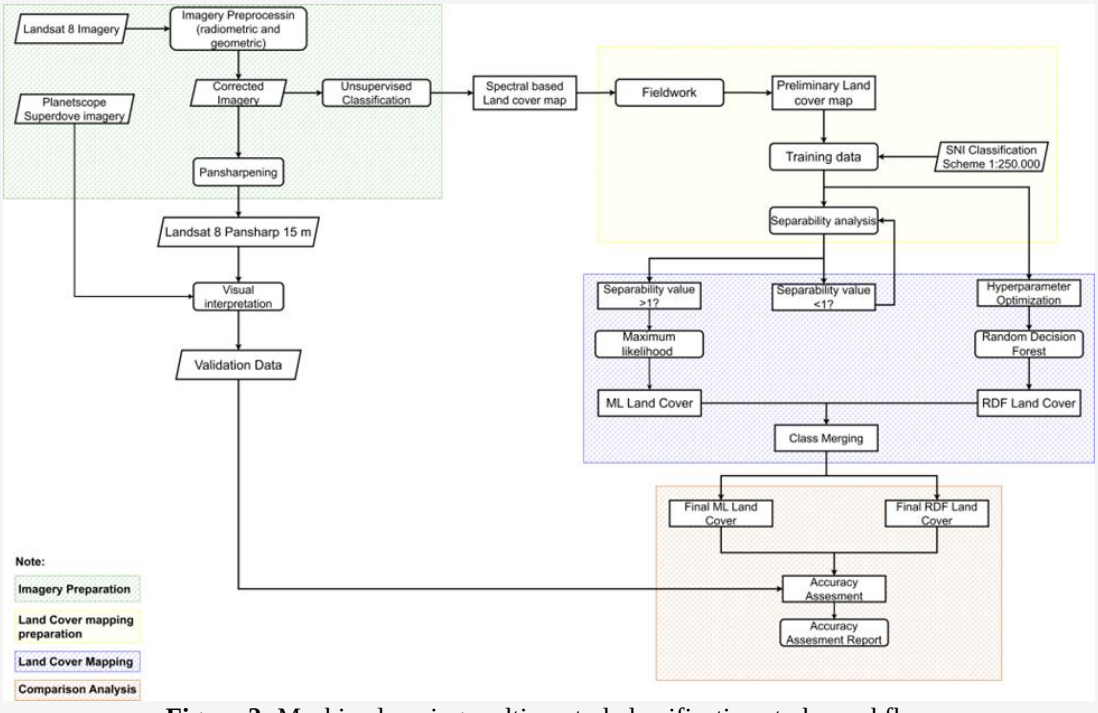

Figure 2: Machine learning multispectral classification study workflow

2.2 Landsat 8 Consideration and Band Selection

Landsat 8 OLI/TIRS collection 2 level 2 TOA imagery recorded in June 2023 is the main data source for this research. We used the VNIR-SWIR (band 1-7) and thermal (band 10) spectrum as input for the classification. This research will only use multispectral bands for the classification in order to fully understand the capability of image classification in mapping detailed land cover. The use of all multispectral band also align with the finding of [18], which concluded that all spectral bands achieve highest accuracy compared to only few bands combination. In addition, parametric algorithm cannot handle multi-source data therefore, only multispectral data will be used, making the input variable equal for both algorithms.

We employed the various spectrum in Landsat 8 to add more spectral reflectance information for better classified the land cover. Coastal aerosol and blue band were used for enhancing water body extraction due to its narrow spectrum [19]. In addition, several type of water body need to be separated in SNI classification scheme therefore, the inclusion of these bands are crucial. NIR and SWIR spectrum are crucial for separating vegetated, and non-vegetated land cover, as demonstrated by [20]. Thermal bands are capable to give additional information for separating various land cover since it is less correlated with other bands [21].

Given that we utilized the 30 meter Landsat 8 OLI/TIRS imagery, we selected a scale of 1:250000 within the SNI classification scheme. A minimum mapping unit (MMU) of 90x90 m (3x3 pixels) is chosen, allowing the identification of smaller land cover in the research location [22]. The appropriate scale of the 30 m Landsat 8 data is 1:60000, derived from equation 1 proposed by [23]. Consequently, the 1:25,000 or 1:50,000 scales are more appropriate, as they better align with Landsat's spatial resolution. However, adopting this scale in SNI classification scheme introduce more challenges since it mixed the land use and land cover classes given that the scheme was originally design for visual interpretation. For instance, at these finer scales, the classification subdivides upland forest into several class based on its status and density, such as primary high density, primary low density, secondary high density, etc. The differentiation of this class is difficult since vegetation density parameter are utilized in this study. Additionally, non-settlement build-up are detailed into more specific class such as, bus terminal, train station, road networks, etc. Since we only used multispectral band, separation of these classes become highly challenging since they have similar spectral pattern, with the main difference lies in land use rather than spectral variation. According to Equation 1, the map scale used in this study is 1:60000 although the detailed of thematic information used are remains at 1:250,000.

$$MS = 2{,}000 R_p \qquad \text{Equation 1}$$

Where:

MS = Scale of the map

R_p = Spatial resolution in meters

2.3 Preliminary Land Cover Map and Training Data Creation

Before creating the training data, key interpretations of the land cover must be developed [24]. These key interpretations will be determined through fieldwork and a preliminary land cover map derived from unsupervised classification. The Iterative Self-Organizing Data Analysis Technique (ISODATA) will be used to classified the imagery into 50 classes in order to separate various spectral pattern in the imagery. The results of the unsupervised classification will be simplified into 17 classes by overlaying it with Landsat 8 and labeled them based on visual interpretation and local knowledge. For example, the ISODATA classification separate forest into several classes, which labeled as forest 1,2,3 etc. Figure 3 shows the process of identifying various forest classes (Figure 3(a)) when compared with Landsat 8 imagery (Figure 3(b)) and the resulting merging of forest classes (Figure 3(c)).

The resulting 17 classes land cover, referred as preliminary land cover map, will be used as the basis for conducting fieldwork to determine the key interpretation. The binomial probability theory, developed by [25] will be used to determine the number of sample. A total of 212 sample is proportionally allocated for all classes and distributed using a stratified random sampling in order to represent smaller land cover classes. The main goal for the fieldwork is identifying key interpretation and aligning the land cover classes identified via preliminary land cover analysis with the SNI classification scheme. After collecting the fieldwork data, the preliminary land cover map will be overlay again with Landsat 8 imagery, in order to ease the creation of the training data by highlighting the spectral pattern boundaries.

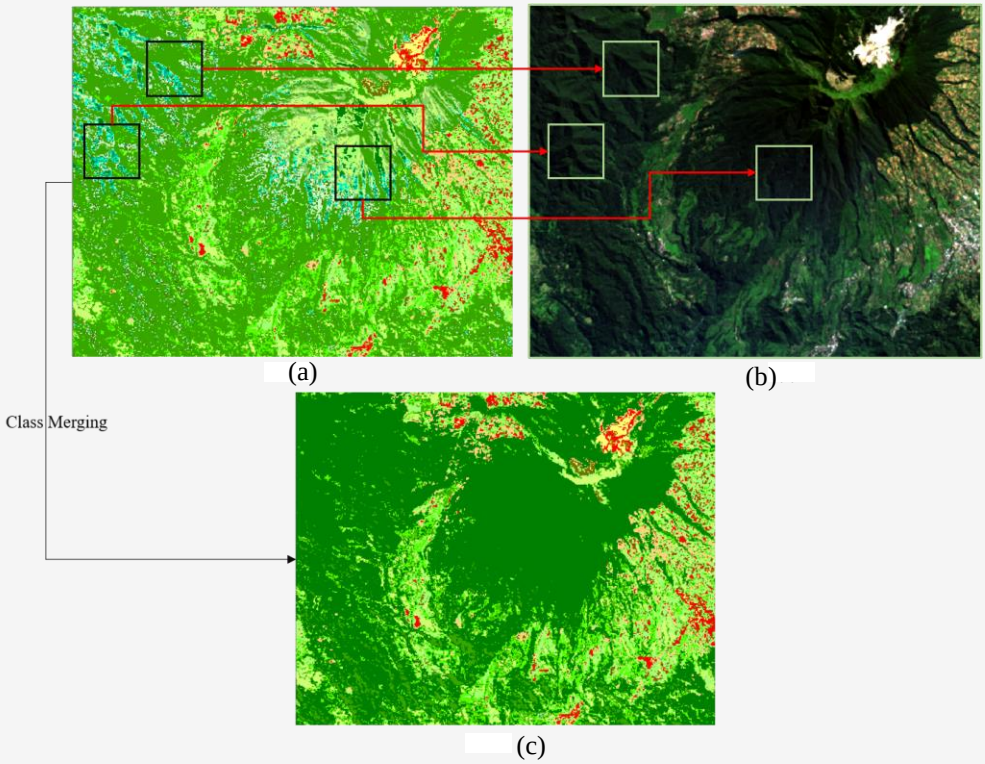

Figure 1: Example of unsupervised classification result:
(a) Comparison with Landsat true color composite (b) indicate that forest is separated into several classes (black and green box), (c)These classes will be merge into single class, resulting in preliminary land cover

2.4 Land Cover Classification

Two commonly used classification algorithm were chosen for representing each approach in digital image classification. The classification using Maximum Likelihood (ML) algorithm will represent the conventional (parametric) classification algorithm since ML were consider as the best algorithm in this approach [15][14] and [26]. Given the limited tools for assessing variable importance in parametric classification, separability analysis is utilized to enhance the quality of training data, ultimately improving the performance of the Maximum Likelihood (ML) algorithm. The Jeffries-Matusita (JM) distance is chosen to assessed the separability of each class in the training data. The JM distance is statistical measure to class separability based on conditional probability theory and measure the average difference between density functions of the two classes [27]. The JM Distance is derived using pooled Mahalanobis distance to measure the mean vectors and covariance structures between two classes. Next, the Bhattacharyya distance (B) is added to measure of the similarity of the two covariance matrices [28]. Finally, the JM distance is calculated as in Equation 2.

$$JM = 2(1 - e^{-B})$$

Equation 2

The resulting separability analysis range from 0 (low separability) to 2 (high separability). JM value less than 1 indicate poor class separability and modification of training data is recommended [29]. These adjustments may involve merging classes with low separability values or excluding areas prone to mixed pixels. The prior probability in ML algorithm will not be used, attributed to the limited information of the land cover distribution in the area of interest.

The classification using Random Decision Forest (RDF) or simply called Random Forest (RF) algorithm will represent the performance of nonparametric approach. Several studies reported that RDF yield better result compared to other nonparametric or machine learning algorithm, with minimum model parameters required [16] and [30]. Other studies stated that RDF is more capable to classified more complex land cover therefore, capable to mapped detailed land cover [9]. Based on the aforementioned reason, we used the RDF algorithm to represent the nonparametric approach in this study.

The RDF algorithm were develop to improve the decision tree classifier by generating random trees, in which each tree cast a vote to classified a certain pixels [16] and [31].

Hyperparameter optimization will be applied to select the parameter combination that yield highest out-of-bag (OOB) accuracy. Th optimization is focused on the number of tree (ntree) and number of variable per split (mtry), since the two parameter were significant in the model performance [30] and [31]. The Importance of each parameter for the final classification result will be evaluated using explanatory testing of RDF algorithm. The explanatory testing will be conducted by splitting the training data into testing and validating data, which used for classification in order to gain OOB accuracy. The explanatory testing also highlights the increase or decrease of OOB accuracy when certain variables were excluded from the model.

2.5 Validation Data Creation and Accuracy Assessment

The Gram-Scmidt pan-sharpening method will be used to fused the Landsat 8 panchromatic band and other multispectral bands. The validation data is then derived through visual interpretation of the 15 m Landsat 8, providing clearer spectral boundaries for easier interpretation. PlanetScope Superdove imagery from the same acquisition period will also use to assist for identifying land cover [32]. The same period of recording provides clearer view of the land cover with similar spectral pattern, providing additional judgement for validation data.

The confusion matrix between the validation data and classified maps will be conducted as part of thematic accuracy assessment. The accuracy metrics observed for each classification consist of Overall Accuracy (OA), quantity disagreement (Qt), and allocation disagreement (At). Overall accuracy expressed the proportion of correctly classified pixels divided by the total pixels in the confusion matrix. Quantity disagreement is expressed as the amount of difference between the reference map and the classified map attributed to the less than perfect match in the proportions of the classes [33]. The allocation disagreement expressed as the amount of difference between the reference map and the classified map attributed to the less than perfect match in the spatial allocation of the classes, given the proportions of the classes in the reference and classified map [34].

We decided not to use kappa coefficient since it provides redundant information with the overall accuracy and does not provide additional information for improving classification [35]. Compared to kappa which measure degree of agreement based on a random chance, the quantity disagreement and allocation disagreement measure how much the agreement is less than perfect, providing additional information and guidance regarding the error [36]. The allocation disagreement is further express by Exchange (Et), Shift (St), which further explain spatial allocation of the classes [33]. Exchange refers to the swapping of the pixels in between two classes, with the same quantity. Exchange is the result of pairwise confusion, in which miss classification happens between two class. Shift refers to much complex allocation, where both the quantity and spatial allocation of the pixels are different. Shift is the result of non-pairwise confusion, in which miss classification happens between more than two classes.

3. Result and Discussion

3.1 Land Cover Classes in the Area of Interest

The fieldwork conducted in May 2024 successfully identified 18 land cover classes in the research location which correspond to the SNI classification scheme. Some of these classes were not initially identified in the preliminary land cover analysis and were only identified following fieldwork and the subsequent creation of training data. The number of classes identified differs from the SNI classification scheme, as some classes listed in the scheme were not present in the study area. Moreover, some other classes in SNI classification scheme had to be combined because difficulties in mapping them using single date imagery. For example, the SNI classification scheme divides croplands into multiple categories, consisting of annual crop, seasonal crop, mixed crops, dryland crops, crops mixed with build-up, and cyclical shifting crops. These types of crops are difficult to classified based on single date imagery, especially annual, seasonal, and cyclical shifting crop, which require temporal imageries to effectively identified and classified them. In addition, without additional data such as soil and topographical data, these classes cannot effectively classify into separate classes. Consequently, the various croplands are combined into single class refer as agricultural land (LP). While this adjustment reduced the land cover detail required by the SNI classification scheme, it was deemed necessary to account for the limitation of digital image classification and increasing the chance of achieving higher accuracy.

Some land cover class also have different spectral pattern although they have the same land cover type. For example, rice field have several spectral patterns depend upon the stage of growth. Figure 4 shows the different spectral response of rice field in different stage of growth.

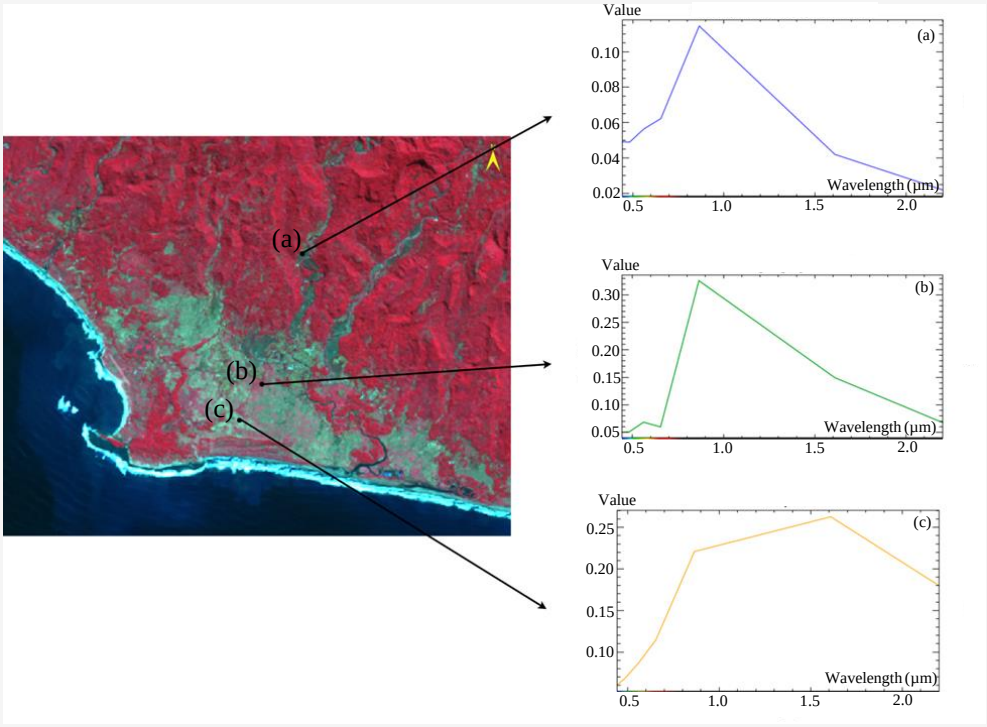

Figure 4: Spectral profile of rice field in different stage of growth viewed through false infrared composite of Landsat 8 (a) recent stage (b) growing stage (c) harvested stage

When the rice is recently planted, the dominant spectral response is water, therefore it shows a much darker color when viewed through false color infrared (Figure 4(a)). If the rice is in the growing stage, the dominant spectral response is green vegetation, therefore it shows a reddish color when viewed in false color infrared (Figure 4(b)). When the rice has been harvested, it shows a much brighter yellow-brownish color in false color infrared (figure 4c). Other example is seen in upland forest class. Two spectral responses for upland forest were identified, first was the forest that were located in valleys, which were not illuminated by the sun and the second is forest that were illuminated. The forest who are not illuminated tends to be darker than the one who are illuminated.

The different spectral pattern increasing the chance of miss classification due to similarity its between classes. For instance, newly planted rice fields may exhibit similar spectral patterns to rivers or water bodies, as since the dominant background reflectance are water. To achieve better separation, 29 classes of training data were created, each based on distinct spectral pattern. These classes will be merge or simplify in the post classification process into 18 classes as identified through fieldwork. The class merging will ignore the spectral pattern of the class and instead focus on the type of the land cover (e.g forest, agricultural land etc). This simplification could contribute to increase the accuracy of land cover classification while also reducing the possibility of the salt-and-pepper effect, which is common problem with pixel-based classification [37]. However, this approach could reduce the level of detail required by SNI classification scheme, although improving the accuracy of the land cover map remain the main focus of this study.

Figure 5 shows the example of initial 29 class land cover map (Figure 5(a)) and its simplification into a final land cover map (Figure 5(b)). The initial land cover shows three type rice field, recently harvested rice field labeled as SWG, growing rice field (vegetated) labeled as SWH, and harvested rice field labeled as SWC. These type of rice fields were merge into a single rice field class (labelled as SW) in the final land cover map. Other example is ocean waters were classified into two type, waves (labeled as OMK) and ocean waters (labeled as PL). Figure 3 clearly shows waves and ocean have two different colors, indicate different spectral pattern. Although waves are not object of land cover, since it is clearly visible in the imagery, the object will be separated, increasing a chance for better separation. The simplification of the initial land cover creates a smoother border between classes. Table 1 shows the 29 classes of land cover and their simplification into 18 classes of land cover along with their corresponding code to simplify their mentioning.

Table 1: Initial and final land cover classes based on SNI classification scheme at the scale of 1:250,000

Initial Land Cover	Initial Land Cover Code	Initial Color Code (RGB)	Simplify Land Cover	Final Land Cover Code	Final Color Code (RGB)
Aquaculture	KAA	250,190,232	Aquaculture	KAA	250,190,232
Man-made Open Field	LTD	255,190,190	Man-made Open Field	LTD	255,190,190
Harvested Agricultural Land	LPK	205,205,102	Agricultural Land	LP	209, 255,115
Recently Planted Agricultural Land	LPC	209,255,115			
Growing Agricultural Land	LPH	137,205,102			
Scrubs and Bushes	SB	116,255,116	Bushes	SB	0,168,132
Herbs and Grass	HR	204,255,204	Herbs and Grass	HR	211,255, 190
Palm Oil Plantation	PBKS	122,245,202	Hardwood Plantation	PBK	137,205,102
Rubber Plantation	PBKK	102,205, 171			
Tea Plantation	PBKT	194,168, 87			
Natural Open Field	LTA	115,115,0	Natural Open Field	LTA	115,115,0
Cloud	AW	255,255,255	Cloud	AW	255,255,255
Growing Rice Field	SWH	168,168,0	Rice Field	SW	168,168,0
Recently Planted Rice Field	SWG	153,99,0			
Harvested Rice Field	SWC	245,245,122			
Natural Freshwater	TA	235,78,68	Natural Freshwater	TA	235,78,68
White Sandy Beach	HPPC	255,235,190	Sandy Beach	HPP	255,211,127
Dark Sandy Beach	HPPG	230,152,0			
Natural/Semi Natural Vegetation Cover	LVA	152,230,0	Natural/Semi Natural Vegetation Cover	LVA	152,230,0
Rocky Fields	HB	137,68,68	Volcanic Rocks and Sands	HB	137,68,68
Natural Volcanic Sands	PA	168,0,132			
River	SI	190, 232,255	River	SI	190,232,255
Non-settlement Build Up	BBP	255,85,0	Non-Settlement Build Up	BBP	255,85,0
Settlement Build Up	BP	255,0,0	Settlement Build Up	BP	255,0,0
Dark Upland Forest	HLTG	38,115,0	Upland Forest	HLT	38,115,0
Illuminated Upland Forest	HLTC	0,168,132			
Coral Reef	TR	160,160,255	Ocean Waters	PL	0,0,255
Ocean Waters	PL	0,0,255			
Waves	OMK	190,210,255			

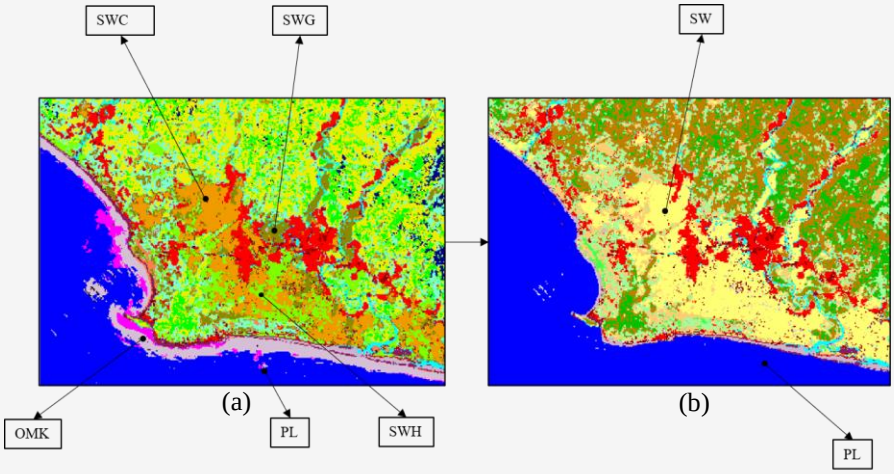

Figure 2: Classified land cover (a) initial land cover (b) final land cover

The land cover type for the SNI classification scheme as shown in Table 1, could be group into three main types, vegetated, water bodies, and non-vegetated land. For the vegetated land, it consists of upland forest (HLT), bushes (SB), natural open field (LTA), semi-natural vegetation (LVA), agricultural land (LP), herbs and grass (HR), rice field (SW), and hardwood plantation (PBK). This vegetated lands mixed both natural land cover (HLT, SB, LTA, LVA, HR) and those who are the result of human intervention (PBK, LP, SW). For the hardwood plantation, SNI classification scheme stated that it encompassed various type of plantation, in which the one who are found in the research location are palm oil, rubber, and tea.

Four water body related land cover were also identified, including aquaculture (KAA), river (SI), natural freshwater body (TA), and ocean waters (PL). These water bodies type have different dominant background (bright-silver material, soil, vegetation), making them possible to be separated through image classification. In addition, different dept of each water body type could increase the potential of classifying them. The non-vegetated land classes consist of non-settlement build up (BBP), settlement build up (BP), volcanic rocks and sand (HB), man-made open field (LTD), and sandy beach (HPP). Build up land were separated since both classes are made of different materials. Non-settlement build-up usually used zinc material for its rooftop, while settlement build up typically used clay. The different materials of these classes, increase the chance of separating them into different classes. Fieldwork conducted reveal that LTD and LTA have different dominant background. LTD consist of disturb soil, as the result of industrial or mining activities, meanwhile LTA have vegetation in the form of scrubs and grass. In addition, SNI classification also stated that LTA predominantly located in volcanic mountains.

3.2 Training Data Creation

A total of 541 polygons consist of 14692 pixels are used to create the initial land cover with 29 classes shown in Table 1. Figure 6 shows the distribution of the training data in the study location. The coastal areas of the location present a more complex land cover, therefore more training data is created in that region. Meanwhile, the center region of the location mostly consists of upland forest, which have a large area and therefore does not require large and distributed number of training data. It should be noted that the training data are not equally or proportionally distributed across all classes, since different size of the classes are identified in the research location. For example, training data for natural freshwater body (TA) were relatively smaller compared to rivers (SI), since the quantity of TA are smaller compared to SI.

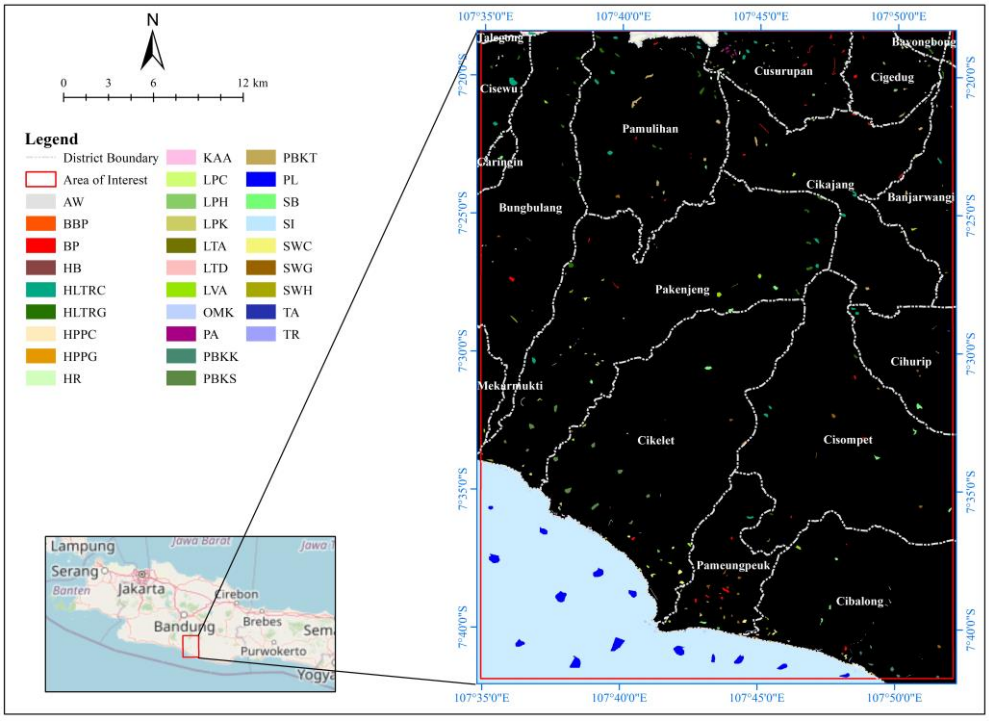

Figure 6: Distribution of the training data in the research location

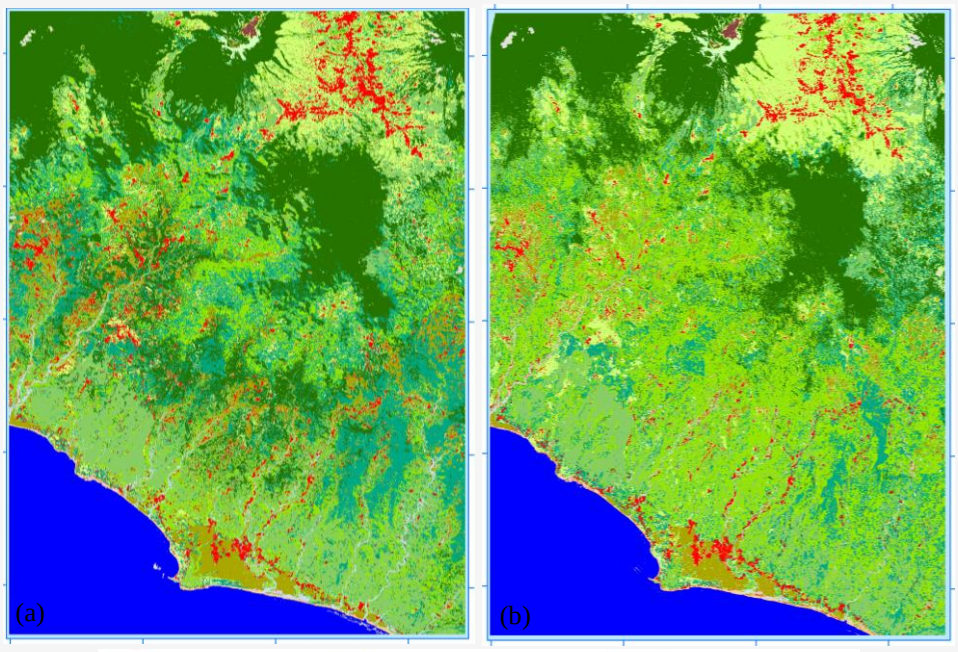

Figure 3: The final land cover classification derived from different classifiers (a) Random Decision Forest (b) Maximum likelihood

Separability analysis shows that all of the classes in the training data have JM value of >1, therefore it did not required modification. The lowest JM value is between the class of natural/semi natural vegetation (LVA) and illuminated upland forest (HLTC), which shows JM value of 1.4. The reason for this low separability value is due to the fact that both classes have similar vegetation type. The only difference is that natural/semi natural vegetation covers usually have high anthropogenic disturbance, thus located near settlement or agricultural land.

3.3 Land Cover Classification Result

The 18 classes land cover map created by both ML and RDF algorithm are shown in Figure 7(b) and Figure 7(a), respectively. The class merging process produced more blocky appearance compared to typical pixelated output of digital image classification. Although the class merging produced blockier result, salt-and-pepper effect is still noticeable when zooming in on certain region. While majority filtering could reduce this effect, it was not utilized in this study due to the presence of smaller land cover classes, such as natural open fields (LTA) and man-made open fields (LTD). Visually, both map shows nearly similar result, although discrepancies are evident in certain areas, particularly in the coastal and mountainous regions. Notably, in the central part of research location, RDF classified the region as bushes (malachite green) and upland forest (dark green), whereas ML classified the same region as semi-natural vegetation (macaw green).

Percentage of each land cover area from both maps shows a quite different result (Figure 8). Largest difference between two algorithm is in the herb and grass class (HR). Other classes also significant difference between ML and RDF, notably rice field (SW), bushes (SB), natural vegetation (LVA), and upland forest (HLT). In ML algorithm, the different area in classes of SB, HR, and PBK are classified as LVA. The possible cause of this difference is that the nonparametric approach assumed normal distribution of the data. This approach employs each class's mean and covariance to calculate the likelihood that a given pixel belongs to a specific class.

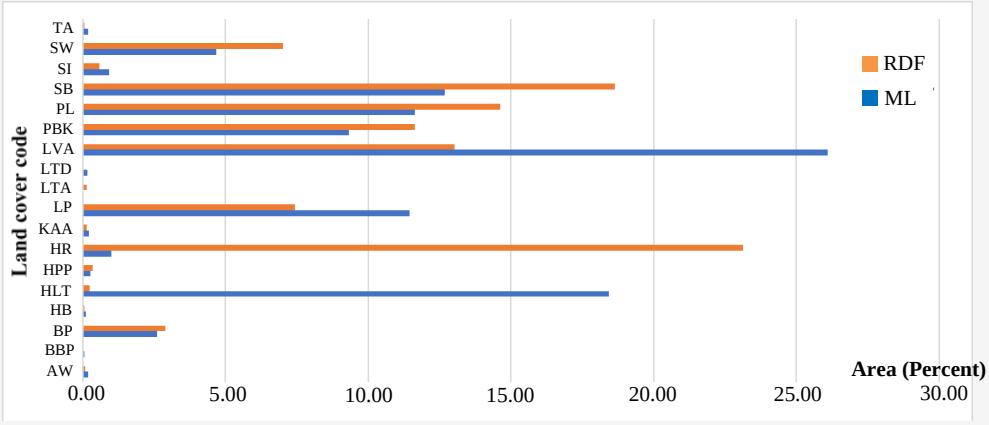

Figure 4: Area percentage of each class in both ML (blue) and RDF (orange) land cover maps

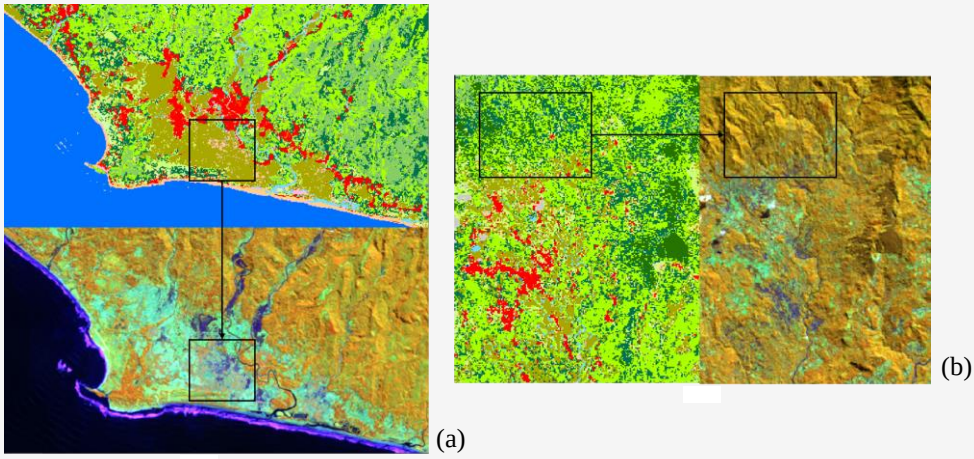

Figure 9: (a) Classification errors in rice field and aquaculture and salt and (b) pepper effect

If the actual data distribution deviates significantly from normality, possibility of miss-classification increase, resulting in differing coverage percentages. LVA are one such class that could be normally distributed, since it refers to vegetation which are similar to HLT, but with higher human intervention, such as agricultural activity conducted between the trees. On the other hand, parametric approach such as RDF, did not make assumption of the data, and use multiple decision tree to classify the pixels, therefore it can handle a much complex data distribution. The complex decision making of RDF algorithm makes it possible to handle mixed pixels, therefore produce a more reliable classification.

3.3.1 Maximum likelihood

As mentioned before, the prior probability of land cover in ML algorithm remain default. Utilizing prior probability can enhance the accuracy of results by assigning higher probabilities to more prevalent land cover types, rather than to those less common [38]. However, the limited availability of similar studies in the research location constrains the understanding of land cover distribution. Other data such as land cover map by the government lacks the necessary detailed and newness that this research require, therefore cannot be used as reference for determining the prior probability. Visual inspection of ML land cover in Figure 9(b) shows an interesting result. The simplification of initial land cover has created a blocky segment instead of pixelated segment. The blocky segment is observed in the classes that originally separated into several classes. The separation based on land cover spectral pattern have successfully mapped land cover with various spectral response. Several miss classifications identify when comparing the original imagery and land cover map. Example are shown in Figure 9(a), which shows the miss classification of rice field into aquaculture.

The miss classification of these classes can be attributed similar spectral response of recently planted rice field and aquaculture, since both had water as the dominant background. Aquaculture is one of the causes that resulted in many miss-classification or salt and pepper effect due to the fact that it had the properties of water and sand. In addition, salt and pepper effect were clearly visible between LVA and HLT classes (Figure 9(b)). This effect between the two classes could be result of the small separability value between the two classes. Since ML algorithm assumes normal distribution of the data, in which are not the case of complex land cover classification. This complexity could infer from the low separability value between LVA and HLT. Therefore, miss classification in this algorithm are highly prominent.

3.3.2 Random decision forest

The hyperparameter tuning process used the explanatory testing that involve in splitting the training data randomly. The 70% of the data will be used to train the model, while the 30% will be used to evaluate the model. The parameter combination that resulted in the highest OOB accuracy is 500 ntree and 4 mtry, with the OOB accuracy of 84.75%.

It should be noted that OOB relates to the stability of model in classifying the data, not the thematic accuracy of the land cover map, and therefore not used as a metric of comparison [9]. One of the advantages of nonparametric/machine learning approach is that the assessment of the contribution of each input parameter in the final model classification. This assessment allows the user to select the most important variable in the classification. Figure 10 shows the contribution (explanatory power) of each input bands in OOB accuracy.

Based on Figure 10, removal of the thermal band (B10) in Landsat 8 result in highest decrease of accuracy, signifies that this band is the most influential band in the model. Band 3-6 shows minimal influence for the performance of the classification. Correlation analysis in the Table 2 shows that thermal band is the least correlated band compared to other bands. Low correlation is also shown by SWIR II band (B7) which align with the decrease of accuracy in Figure 10. In contrast, removing the blue band (B2) contribute in the increase of OOB accuracy. It should be noted that spectral bands are tend to correlate will its nearby spectrum, therefore the VNIR spectrum shows high correlation value between each band.

Table 2: Correlation analysis between Landsat 8 multispectral bands used in this study

	B1	B2	B3	B4	B5	B6	B7	B10
B1	1							
B2	0.989523	1						
B3	0.851953	0.900695	1					
B4	0.782601	0.847395	0.953814	1				
B5	-0.2089	-0.18035	0.178533	0.107835	1			
B6	-0.13181	-0.08214	0.291312	0.317098	0.852525	1		
B7	-0.01069	0.051935	0.373359	0.473017	0.595047	0.913201	1	
B10	0.518101	0.465527	0.458821	0.413879	0.176925	0.329345	0.397397	1

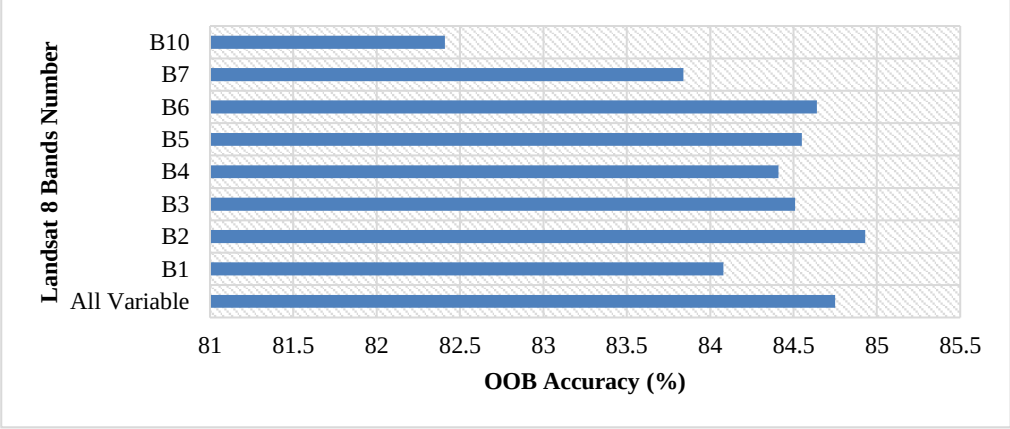

Figure 10: Explanatory power of each band resulting in decrease or increase of OOB accuracy

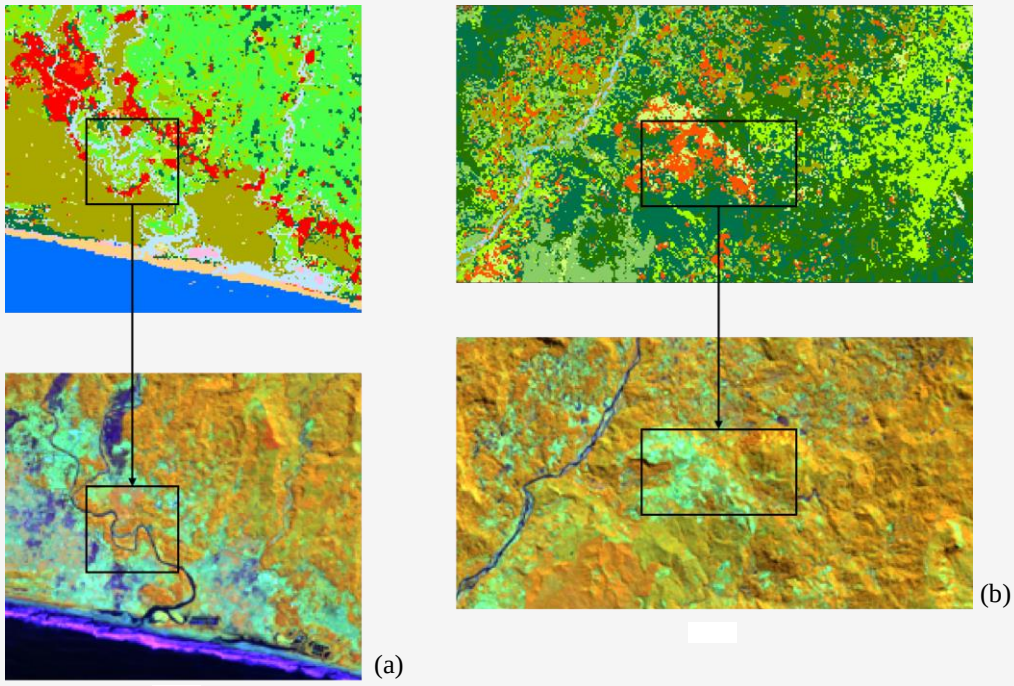

Figure 11: Miss classification in RDF classifier, (a) river and rice field agricultural land and (b) urban areas

Since comparison with ML algorithm which included all the spectral bands, the same input will be used for the RDF classification. Several miss-classification also detected in RDF land cover map, example of them is shown in Figure 11. The miss classification happened between rivers - rice field (Figure 11(a)) and build-up – agricultural land (Figure 11(b)). The miss-classification between rivers and rice fields can be caused by local resident habit of planting rice close to rivers. The spectral response of both objects can be similar especially when the rice is still recently planted. Similarly, many residents also planted crop and other plantation near or around settlement. Therefore, resulted in mix spectral response and pattern of both land cover, especially newly planted agricultural land, which usually cover with silver colored tarp. Although miss-classification is found, thematic accuracy assessment will be conducted to fully evaluated the quality of land cover product.

3.4 Accuracy Assessment

Visual interpretation for the validation data resulted in 336 polygons encompassing 23539 pixels, that will be used for accuracy assessment. This data is created separately with the training data in order to produce an independent validation dataset. The independent validation dataset is crucial to create an unbiased accuracy assessment report. As mention in section 3.2, the validation data are not proportionally distributed across the land cover class due different class size of the land cover in the area of interest. The smaller land cover class consist of non-settlement build up (BBP), natural freshwater body (TA), aquaculture (KAA), and man-made open field (LTD). Since some of these classes are used for creating the training data, interpreting other location that can be used for the validation data is a difficult task, therefore resulting in imbalance validation data. The distribution of the validation data is shown in Figure 12.

3.4.1 Accuracy metrices

The RDF land cover map achieved an overall accuracy (OA) of 82.92%, while the ML land cover map resulted in an OA of 81.67%. The OA values between these two algorithms show little difference, although RDF resulted in higher accuracy. The various land cover classes required for this study certainly resulted in difficulties for both algorithms to effectively separate them. Per-class accuracy metrics will produce a more detailed information for comparison of both algorithms. The quantity and allocation disagreement produce a more complex metrics for assessing overall performance and class specific performance. Based on Figure 13, ML land cover map resulted in lower quantity disagreement (50.6%) compared to the RDF land cover map (77.7%). On the other hand, RDF land cover map resulted in lower allocation disagreement (22.2%) compared to ML land cover map (49.3%).

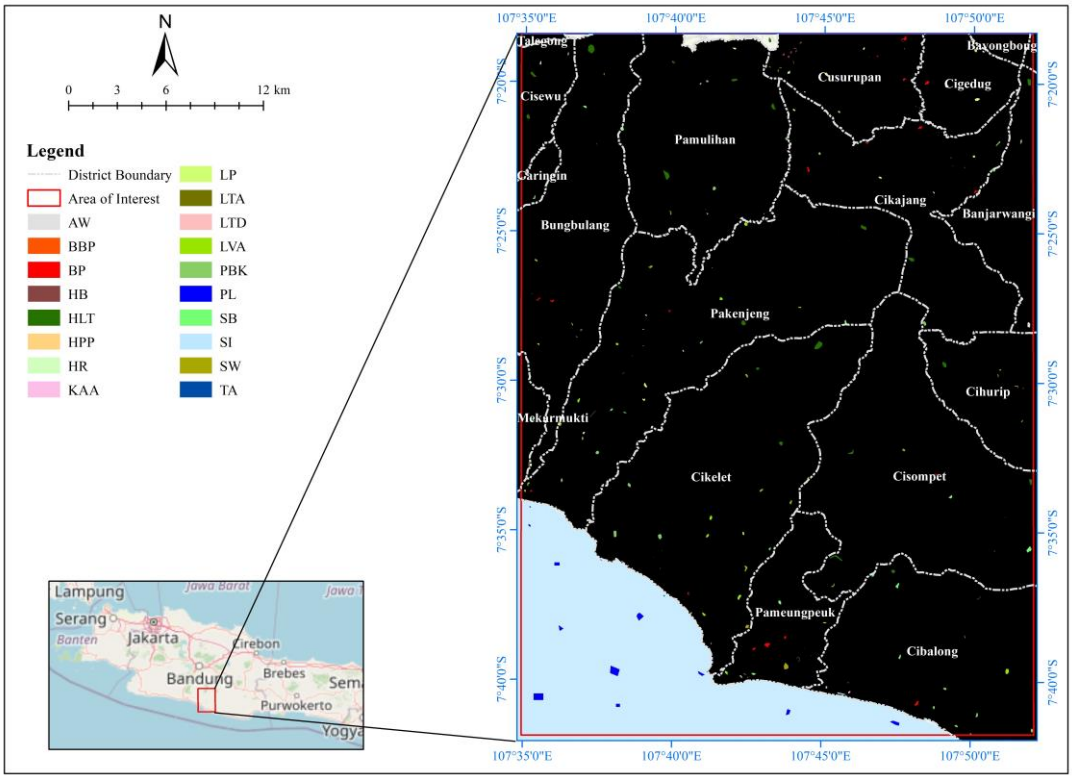

Figure 12: Distribution of the validation data for accuracy assessment report

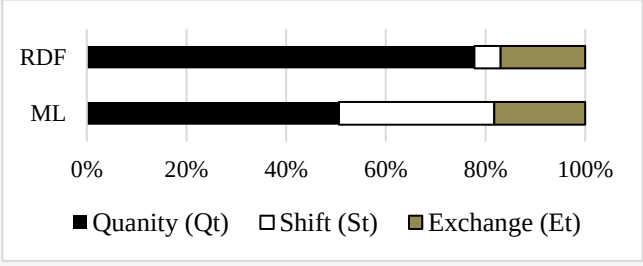

Figure 13: Comparison of two classifiers quantity disagreement (quantity) and allocation disagreement (Exchange and shift)

Quantity disagreement is the largest disagreement in the RDF map, signify that RDF either overestimate of underestimate the land cover class proportions. The smaller allocation disagreement indicates that most of the over or under estimated class are spatially correct.

Although ML land cover map has smaller quantity disagreement, the large allocation disagreement signifies that the total quantity of the reference pixels is better than RDF, but many of them are spatially incorrect. The exchange and shift component indicate inter-class miss classification, in which exchange indicate pairwise miss-classification, and shift, indicate non-pairwise miss classification. The ML land cover map shows higher exchange component, signifies that most of the miss classification happens due to pairwise miss classification (between two classes). Meanwhile, shift component indicates miss-classification between more than two classes, which also observed in both RDF and ML land cover map. Disagreement between classes are present in the form difference class intensity, as proposed by [39]. Class difference intensity is computed by considering various different class size and present them in percentage for easier interpretation. Figure 14 shows each class component's contribution towards the overall quantity and allocation disagreement by presenting in each category's intensity and overall intensity for both land cover maps.

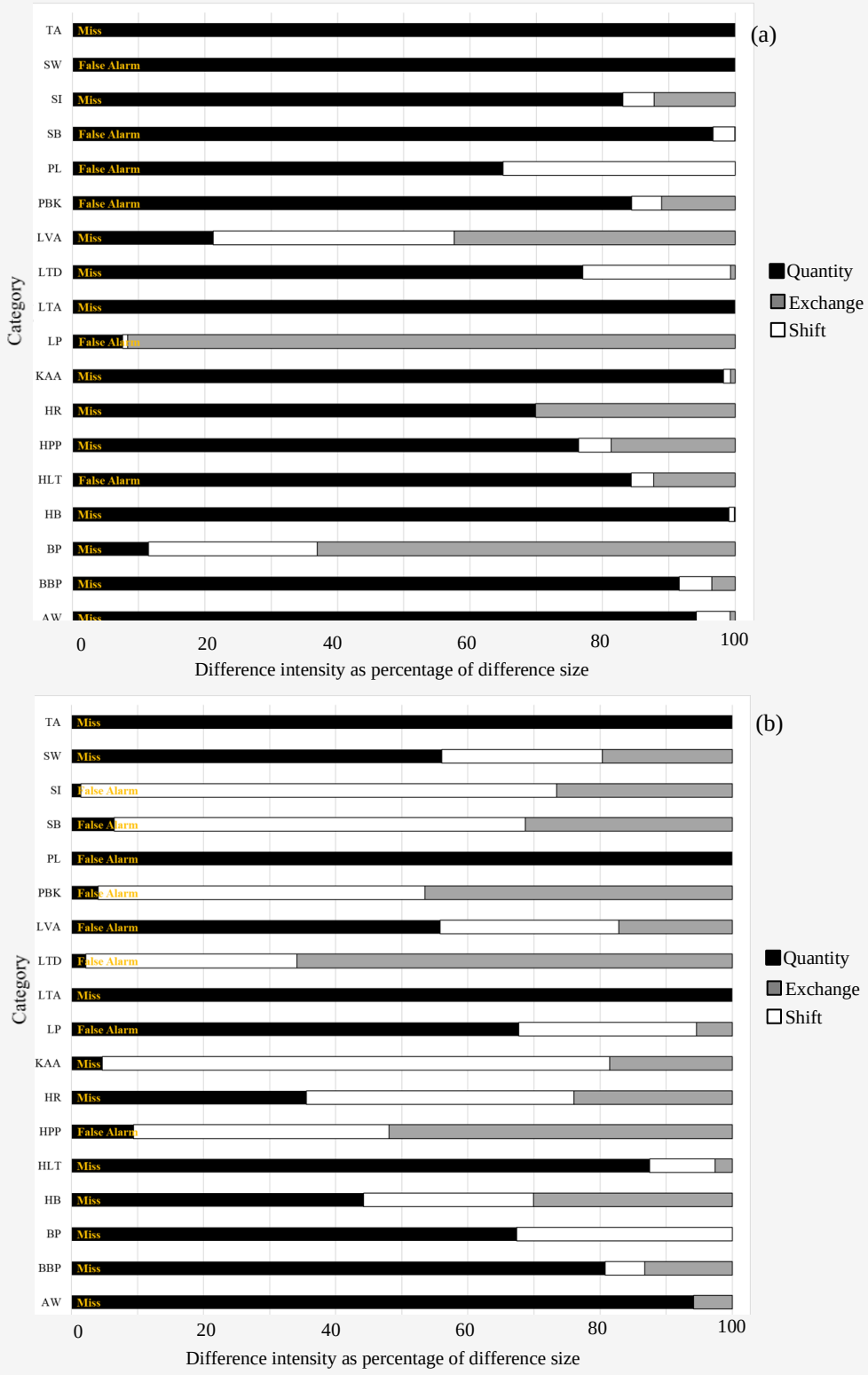

Figure 14: (a) Class intensity disagreement for ML land cover map and (b) RDF land cover map

For the ML land cover map (Figure 14(a)), aquaculture (KAA), man-made open field (LTD), bushes (SB), hardwood plantation (PBK), and rivers (SI) account the largest shift and exchange difference. The class labels indicate commission (false alarms) error and omission (miss) error. The

exchange component of KAA account for approximately 80% of the difference in the class. Signifies that this class is more extensively miss-classified compared to allocation disagreement. The large exchange component also shows that this class are confuse between other class, possibly river, which shows the similar pattern. The shift component of LTD is more extensive than other class, indicate that these classes are miss-classified with more than two class, most likely between LP, BBP, and BP classes, indicated by the large quantity difference between these classes. The higher allocation disagreement could be reduced by aggregating the classes which resulted in higher exchange and shifts.

The difference higher quantity disagreement of the classes in the RDF land cover map (Figure 14(b)) indicates spatial context of quantity disagreement happened. The agricultural land (LP), rice fields (SW), upland forest (HLT), non-settlement build up (BBP), and settlement build up, account for most quantity disagreement for RDF land cover map. LP accounts for most exchange difference, in which these exchanged happened with cloud (AW). The primary source of these exchange could be attributed to newly planted agricultural land, which usually have similar spectral pattern with cloud. Rice field (SW), natural open field (LTA) and natural freshwater (TA) shows no allocation disagreement, indicate that RDF underestimate the quantity of these class. Improving the quantity of these class should be conducted by adding multi-source data that could improve the resulting quantity of these class.

3.4.3 Discussion

Other studies shows that visual interpretation using SNI classification scheme for land cover/land use (LULC) mapping achieve higher accuracy compared to this study. One of the study manage to achieve >90% accuracy with 1:50.000 LULC map [24]. It should be noted that the area of interest is significantly smaller than the location in this study. Other study produced LULC maps with the accuracy of 80.75% with 52 classes and 88.7% with 32 classes [6]. This study also used the 1:50.000 scale for its LULC map, with the 15 m Landsat 8 as the basis for visual interpretation while applying the landscape ecology approach. On the other hand, some study also implemented digital image classification while using modified version of SNI classification scheme [40]. This study conducted several simulation using Multilayer Perceptron (MLP) classifier and achieve the average accuracy of >75%. In comparison with this study, the approach implement manage to achieve higher accuracy with more detailed classes. Implementation of digital image classification for SNI classification remain limited, in which separating mutually exclusive classes remained a challenge for many classifications algorithm. Spectral pattern similarity also resulted in difficulties in creating adequate separation between the classes. The approach in this study could mitigate the difficulties in mapping land cover with similar spectral pattern.

The quantity disagreement and allocation disagreement reveal different result for both land cover maps. The larger allocation disagreement in ML land cover indicated less accurate land cover, considering the spatial allocation of the pixels. The RDF land cover map has smaller allocation disagreement, with higher quantity disagreement. Class level disagreement indicate that most classes are overestimate, indicate that although the spatial allocation are correct, the quantity are not. The accuracy metrics also reveal further information which are not possible to interpret from the percent correct metrics. The ML algorithm is more capable to resulted in land cover with smaller quantity disagreement, indicate that ML did not tend to overestimate the result. On the hand, the RDF land cover could result in an over or under estimate land cover, but with better spatial allocation. The class level disagreement provides information of the exchange and shift between class with respect of the overall class size. Based on this information, improvement classification performance can be deduced. For example, ML land cover map allocation disagreement could be reduced by combining the KAA and SI class, since both classes shows higher exchange disagreement.

When comparing the overall accuracy, nonparametric classification resulted in higher accuracy, although the difference is relatively small in this study. Limitation of parametric classification, especially when handling complex land cover and classification scheme contributed into higher allocation disagreement as shown in this study. In addition, imbalance training and validation data were a significant limitation encountered in this study. RDF are more capable to handle such conditions, in which the ML algorithm could not. Based on previous studies, it is noted that visual interpretation still achieves higher accuracy while using more detailed classification scale.

When considering the limitation of digital image classification and the used of single date multispectral data only, the accuracy achieved in this study are consider sufficient. Although for practical implementation, this accuracy is not significant enough and improvement should be made by incorporating additional information such as topographical data, spectral indices, textural, and other GIS data.

5. Conclusion

This study conducted a detailed land cover mapping based on spectral information from Landsat 8 OLI/TIRS while using the SNI 7645-1 classification scheme with the scale of 1:250.000. Implementation of preliminary land cover map and fieldwork successfully identified 18 land cover classes that are aligned with SNI classification, although modification to some classes is needed. Due to various spectral pattern identified, 29 classes of initial land cover were created in order increase the chance to separate these spectral patterns. The initial land cover map will be simplified through class merging into the final land cover map which contain 18 classes. Through this approach, various spectral pattern is successfully classified creating more blocky land cover appearance compared to the typical pixelated result of pixel-based classification.

Thematic accuracy assessment of two land cover maps created in this study, shows that RDF land cover map resulted higher OA accuracy. The allocation disagreement for this algorithm is significantly lower compared to ML, although overestimation of the land cover classes is detected. On the other hand, the ML land cover map shows lower quantity disagreement, indicating that in term of quantity, the land cover in ML land cover map produced a better land cover map, although higher miss-classification is higher, indicate by the higher allocation disagreement. The result in this study aligned with many studies regarding digital image classification for land cover mapping. Nonparametric approach is known for is capability to handle complex land cover, this study reiterate that this approach can also handle complex classification scheme. Although the accuracy achieve are acceptable, further efforts should be made to increase both quantitative and qualitative quality of the land cover map. This study provided alternative approach for land cover mapping using SNI classification scheme, which were design for visual interpretation. This approach can be considered when rapid land cover data is needed for other applications. This approach also served as alternative when additional data for accurate visual interpretation are not accessible.

Acknowledgement

This research was supported by the 2024 Lecturer Independent Research Program assigned to Muhammad Kamal, funded by the Faculty of Geography at Universitas Gadjah Mada, Indonesia with the grant number of 304/UN1/GE/KPT/2024.

References

[1] Cihlar, J., (2000). Land Cover Mapping of Large Areas from Satellites: Status and Research Priorities. *International Journal of Remote Sensing*, Vol. 21(6-7), 1093–1114. https://doi.org/10.1080/014311600210092.

[2] Loveland, T. R., (2012). History of Land Cover Mapping. In *Remote Sensing of Land Use and Land Cover: Principle and Application*, 1st ed. C. P. Giri, Ed. New York: Taylor and Francis.

[3] Phiri, D. and Morgenroth, J., (2017). Developments in Landsat Land Cover Classification Methods: A Review. *Remote Sensing*, Vol. 9(9). https://doi.org/10.3390/rs9090967.

[4] Danoedoro, P., Phinn, S. and McDonald, G., (2004). Developing a Versatile Land-Use Information System Based on Satellite Imagery for Local Planning in Indonesia Phase I: Establishment of Classification Scheme. *GISDECO 2004: 7th Seventh International on GIS in Developing Countries*, *May 2004*, 10–12.

[5] Putri, E. A. W. A., Danoedoro, P. and Farda, N. M. M., (2019). Comparing Land-Cover Maps Accuracies Generated from Multispectral Classification of Landsat-8 OLI and Pleiades Images Using Two Different Classification Schemes. *Proc. SPIE 11311, Sixth Geoinformation Science Symposium,* Vol. 11311. https://doi.org/10.1117/12.2548888.

[6] Danoedoro, P., Ananda, I. N., Kartika, C. S. D., Umela, A. F. and Indayani, A. B., (2020). Testing a Detailed Classification Scheme for Land-Cover/ Land-Use Mapping of Typical Indonesian Landscapes: Case Study of Sarolangun, Jambi and Salatiga, Central Java. *Indonesian Journal of Geography*, Vol. 21 52(3). https://doi.org/10.22146/ijg.50080.

[7] Dwiputra, A. J., Suharyadi, R. and Danoedoro, P., (2016). Pengaruh Jumlah Kelas dan Skema Klasifikasi Terhadap Akurasi Informasi Penggunaan Lahan Hasil Klasifikasi Berbasis Objek Dengan Teknik Support Vector Machine di Sebagian Kabupaten Kebumen Provinsi Jawa Tengah [Effect of Number of Classes and Classification Scheme on Accuracy of Land Use Information from Object-Based Classification with Support Vector Machine Technique in Part of Kebumen Regency, Central Java Province]. *Majalah Geografi Indonesia*, Vol. 30(2). https://doi.org/10.22146/mgi.15632.

[8] Danoedoro, P., Ananda, I. N., Wulandari, Y., Umela, A. F., Ratnasari, N., Rasyidi, E. S., Pahlefi, M. R., Ramadanningrum, D. P., Kulsum, I. I., Juniansah, A., Tyas, B. I., Rosalina, L. and Narmaningrum, D. A., (2019). Developing Interpretation Methods for Detailed Categorisation-Based Land-Cover/Land-Use Mapping at 1:50,000 Scale in Indonesia. In T. D. Pham, K. D. Kanniah, K. Arai, G. J. P. Perez, Y. Setiawan, L. B. Prasetyo, and Y. Murayama (Eds.), *Sixth International Symposium on LAPAN-IPB Satellite,* Vol. 1137205. https://doi.org/10.1117/12.2541857.

[9] Danoedoro, P., Widayani, P., Hidayati, I. N., Kartika, C. S. D., and Alfani, F. (2024). Incorporating Landscape Ecological Approach in Machine Learning Classification for Agricultural Land-Use Mapping Based on a Single Date Imagery. *Geocarto International*, Vol. 39 (1). https://doi.org/10.1080/10106049.024.2356844

[10] Jensen, J. R., (2015). *Introductory Digital Image Processing: A Remote Sensing Perspective,* 4th ed. New York: Pearson Series in Geographic Information Science.

[11] Malingreau, J. and Christiani, R., (1981). A Land Cover/Land Use Classification for Indonesia. *Indonesian Journal of Geography*, Vol.11(42), 13–47.

[12] Sandy, I. M., (1982). *Penggunaan Tanah (Land Use) di Indonesia* [Land Use in Indonesia]. Jakarta: Badan Pertanahan Nasional.

[13] BSN. (2014). *Standar Nasional Indonesia 7645-1:2014 Tentang Klasifikasi Penutup Lahan Bagian 1 - Skala Kecil dan Menengah* [Indonesia National Standard 7645-1:2014 on Land Cover Classification Part – Small and Medium Scale]. Jakarta: Badan Informasi Geospasial.

[14] Mancino, G., Falciano, A., Console, R. and Trivigno, M. L., (2023). Comparison between Parametric and Non-Parametric Supervised Land Cover Classifications of Sentinel-2 MSI and Landsat-8 OLI Data. *Geographies*, Vol. 3(1), 82-109. https://doi.org/10.3390/geographies3010005.

[15] Lu, D., Weng, Q., Moran, E., Li, G. and Hetrick, S., (2011). Remote Sensing Image Classification. In *Advances in Environmental Remote Sensing: Sensors, Algorithms, and Applications* 1st ed. CRC Press.

[16] Gislason, P. O., Benediktsson, J. A. and Sveinsson, J. R., (2006). Random Forests for Land Cover Classification. *Pattern Recognition Letters*, Vol 27(4), 294–300. https://doi.org/10.1016/j.patrec.2005.08.011.

[17] Pal, M. and Mather, P. M., (2004). Assessment of the Effectiveness of Support Vector Machines for Hyperspectral Data. *Future Generation Computer Systems*, Vol. 20(7), 1215–1225. https://doi.org/10.1016/j.future.2003.11.011.

[18] Yu, Z., Di, L., Yang, R., Tang, J., Lin, L., Zhang, C., Rahman, M. S., Zhao, H., Gaigalas, J., Yu, E. G., and Sun, Z. (2019). Selection of Landsat 8 OLI Band Combinations for Land Use and Land Cover Classification. *2019 8th International Conference on Agro-Geoinformatics (Agro-Geoinformatics)*, 1–5. https://doi.org/10.1109/AgroGeoinformatics.2019.8820595

[19] Aroma, R. J., Raimond, K., Estrela, V. V. and de Jesus, M. A., (2024). A Coastal Band Spectral Combination for Water Body Extraction Using Landsat 8 Images. *International Journal of Environmental Science and Technology*, Vol. 21(2), 1767–1784. https://doi.org/10.1007/s13762-023-05027-z.

[20] Sato, H. P. and Tateishi, R., (2004). Land Cover Classification in SE Asia Using Near and Shortwave Infrared Bands. *International Journal of Remote Sensing*, Vol. 25(14), 2821–2832. https://doi.org/10.1080/01431160310001618400.

[21] Sun, L. and Schulz, K., (2015). The Improvement of Land Cover Classification by Thermal Remote Sensing. *Remote Sensing*, Vol. 7(7), 8368–8390. https://doi.org/10.3390/rs70708368.

[22] Knight, J. F. and Lunetta, R. S., (2003). An Experimental Assessment of Minimum Mapping Unit Size. *IEEE Transactions on Geoscience and Remote Sensing*, Vol. 41(9), 2132–2134. https://doi.org/10.1109/TGRS.2003.816587.

[23] Tobler, W., (1987). Measuring Spatial Resolution. *Proceedings, Land Resources Information Systems*, Beijing, 12–16.

[24] Sari, M. I., Danoedoro, P. and Widayani, P., (2021). Image Interpretation Keys for 1:50.000 Scaled of Land Use Mapping Using Landsat 8 with SNI 7645:2014 Classification. *The 3rd International Conference of Geography and Education*.

[25] Fitzpatrick-Lins, K., (1981). Comparison of Sampling Procedures and Data Analysis for a Land- Use and Land-Cover Map. *Photogrammetry Engineering and Remote Sensing*, Vol. 47(3), 343–351.

[26] Lu, D. and Weng, Q., (2007). A Survey of Image Classification Methods and Techniques for Improving Classification Performance. *International Journal of Remote Sensing*, Vol. 28(5), 823–870. https://doi.org/10.1080/01431160600746456.

[27] Arvor, D., Jonathan, M., Meirelles, M. S. P., Dubreuil, V. and Durieux, L., (2011). Classification of MODIS EVI Time Series for Crop Mapping in the State of Mato Grosso, Brazil. *International Journal of Remote Sensing*, Vol. 32(22), 7847–7871. https://doi.org/10.1080/01431161.2010.531783.

[28] Van Niel, T., McVicar, T. and Datt, B., (2005). On the Relationship between Training Sample Size and Data Dimensionality: Monte Carlo Analysis of Broadband Multi-Temporal Classification. *Remote Sensing of Environment*, Vol. 98(4), 468–480. https://doi.org/10.1016/j.rse.2005.08.011.

[29] Region of Intrerest (ROI) Tool (2023). *ENVI - Environment for Visualizing Images User Guide*. https://www.nv5geospatialsoftware.com/docs/RegionOfInterestTool.html#ROISeparability (accessed Sep. 26, 2024).

[30] Eastman, J. R., (2009). *Idrisi TerrSet – Guide to GIS and Image Processing*. Clark University.

[31] Maxwell, A. E., Warner, T. A. and Fang, F., (2018). Implementation of Machine-Learning Classification in Remote Sensing: An Applied Review. *International Journal of Remote Sensing*, Vol. 39(9), 2784–2817. https://doi.org/10.1080/01431161.2018.1433343.

[32] Planet Application Program Interface: In Space for Life on Earth. *Planet Labs.* Available https://api.planet.com [Accessed May 20, 2024].

[33] Pontius, R. G. and Santacruz, A., (2014). Quantity, Exchange, and Shift Components of Difference in a Square Contingency Table. *International Journal of Remote Sensing*, Vol. 35(21), 7543–7554. https://doi.org/10.1080/2150704X.2014.969814.

[34] Sarmento, E. C., Giasson, E., Weber, E., Flores, C. A. and Hasenack, H., (2012). Prediction of Soil Orders with High Spatial Resolution: Response of Different Classifiers to Sampling Density. *Pesquisa Agropecuária Brasileira*, Vol. 47(9), 1395–1403. https://doi.org/10.1590/S0100-204X2012000900025.

[35] Foody, G. M., (2020). Explaining the Unsuitability of the Kappa Coefficient in the Assessment and Comparison of the Accuracy of Thematic Maps Obtained by Image Classification. *Remote Sensing of Environment*, Vol. 239. https://doi.org/10.1016/j.rse.2019.111630.

[36] Pontius, R. G. and Millones, M., (2011). Death to Kappa: Birth of Quantity Disagreement and Allocation Disagreement for Accuracy Assessment. *International Journal of Remote Sensing*, Vol. 32(15), 4407–4429. https://doi.org/10.1080/01431161.2011.552923.

[37] Hirayama, H., Sharma, R. C., Tomita, M. and Hara, K., (2019). Evaluating Multiple Classifier System for the Reduction of Salt-and-Pepper Noise in the Classification of Very-High-Resolution Satellite Images. *International Journal of Remote Sensing*, Vol. 40(7), 2542–2557. https://doi.org/10.1080/01431161.2018.1528400.

[38] Strahler, A. H., (1980). The Use of Prior Probabilities in Maximum Likelihood Classification of Remotely Sensed Data. *Remote Sensing of Environment*, Vol. 10(2), 135–163. https://doi.org/10.1016/0034-257(80)90011-5.

[39] Pontius Jr, R. G., (2019). Component Intensities to Relate Difference by Category with Difference Overall. *International Journal of Applied Earth Observation and Geoinformation*, Vol. 77, 94–99. https://doi.org/10.1016/j.jag.2018.07.024.

[40] Rini, M. S., (2018). Kajian Kemampuan Metode Neural Network untuk Klasifikasi Penutup Lahan dengan Menggunakan Citra Landsat-8 OLI (Kasus di Kota Yogyakarta dan Sekitarnya). [Assessment of the Capability of Neural Network Method for Land Cover Classification Using Landsat-8 OLI Imagery (Case Study Yogyakarta City and Surrounding Areas)] *Geomedia: Majalah Ilmiah Dan Informasi Kegeografian*, Vol. 16(1), 1-12. https://doi.org/10.21831/gm.v16i1.20974.